

# COMPUTATIONAL METHOD FOR STEADY FLOW (RANS) USING ZONAL APPROACH AND ITS IMPLEMENTATION EXPERIENCE FOR SOLUTION OF TASK OF INTERFERENCE ENGINE AND AIRFRAME

Anisimov K.\*, Kazhan E.\*, Lysenkov A.\*

\*The Central Aerohydrodynamic Institute named after N.E. Zhukovsky, Russia

**Keywords:** *CFD methods, interference engine and airframe, engine air intake*

## Abstract

*The implicit smoother method is developed to accelerate the stationary numerical solution of viscous flow around aircraft by an explicit Godunov–Kolgan–Rodionov scheme. The local choice of an explicit or implicit scheme (zonal approach) and the manner of time step implementation (global or local), depending on the relationship between the specified global time step and the local stability condition of the explicit scheme, is the main specific feature of the numerical method. The developed software is used for research in the following configurations: “over wing”, “over fuselage” and configuration with distributed propulsion placed in a wing.*

## 1 Introduction

The technology for CFD experiments called the electronic aerodynamic wind tunnel (EWT) has been developed and widely applied at TsAGI [1]. The software package *EWT-TsAGI* [2], developed for this technology contains the entire set of instrumentation to implement CFD experiments. CFD experiments enable investigating viscous gas turbulent flows around real configurations, including simulation of real aerodynamic experiments (taking into account experimental facility features). This paper proposes ways to accelerate obtaining stationary solutions within this technology. *EWT-TsAGI* contains several solvers, including the *V3Solver* [3] and *ZEUS* [4]. To obtain stationary solutions the relaxation method is

applied in these solvers, and the steady flow is obtained as a limit of unsteady process. All numerical schemes, which can be used in the relaxation method, may be divided into two classes, namely, explicit and implicit schemes. They have their own pros and cons. The implicit schemes can be absolutely stable, but they require more computational resources per iteration than the explicit ones. Both explicit and implicit numerical schemes are widely applied in CFD and have many implementations [5]. Up to now, only explicit schemes have been used in *EWT-TsAGI*. To accelerate obtaining the stationary solutions, the local time step technique was applied. This means that the computation was performed with different time steps in different cells of the CFD grid. The time steps were determined by the local stability limitations.

Currently, the development of technologies for the "greener" aircraft is in different areas: the creation of engines with better acoustic and emission characteristics, improving the acoustic panel design, the choice of the optimized takeoff and landing trajectory, configurations design with the airframe noise shielding and etc. The requirements to reduce noise and fuel consumption make it necessary to consider the airframe and power plant as an integrated system. For example, a way to radically reduce noise is to use non-traditional integrated layouts. Often, however, new technical solutions to reduce the noise may be contrary to the requirements of improving fuel efficiency and safety by reducing the range of

stable operation of the propulsion. Therefore, for the non-traditional configurations it is necessary to investigate in detail the effects of the integration of a propulsion and an airframe, additional installation losses, as well as the distortions of the flow in front of the turbofan due to flow around the airframe at takeoff and cruise regimes.

The following characteristics are declared in russian and european forecasts of aviation technology development to 2030:

- fuel consumption reduction up to 60%
- NO<sub>x</sub> emission reduction on 80%
- Noise reduction of 30 EPNdB relative to Chapter 4

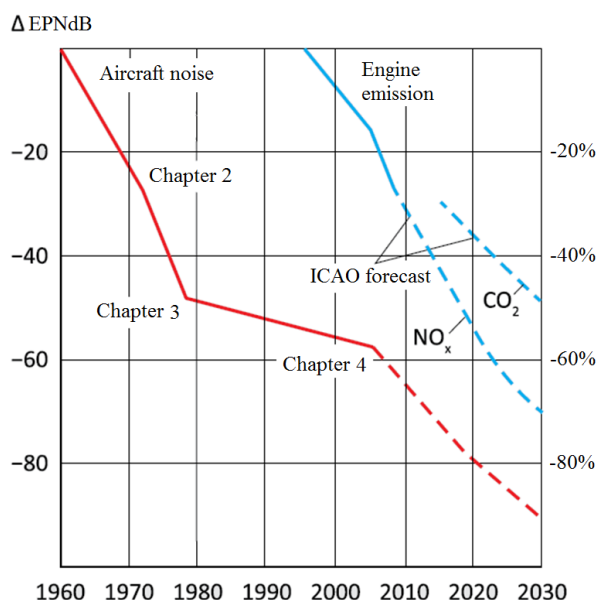


Figure 1 – forecast of noise and emission reduction

Such high performance can be achieved with the implementation of integrated configurations only [Ошибка! Источник ссылки не найден.-Ошибка! Источник ссылки не найден.]. TsAGI investigate many perspective configurations with deep integration of power plant and airframe. Aerodynamic features of a power plant of two configurations are considered in the present paper.

It is necessary to carry out the following objectives for power plant aerodynamics

designing aircrafts (especially integrated configurations):

- Minimal installation losses
- Objectives on flow distortion on engine entrance:
  - absence of a boundary layer separation in the inlet for all working regimes range
  - absence of vortexes in the inlet entrance
  - minimal level of flow distortions in the engine entrance
- Minimal probability of foreign particles hitting
- airfield services convenience

Special attention must be paid to multidisciplinary investigations. For example, flow distortions on the engine entrance have an influence not only on gas dynamics stability power plant working but also on acoustic characteristics of the engine fan.

## 2 CFD tools used

There are two approaches that enable the stationary solution to be obtained faster than in the case of using the explicit scheme with local time step. The first approach is the application of the multigrid methods [6], [7]; another approach is the implicit scheme application. This work deals with the second approach.

Current implicit methods in the solution of CFD stationary problems are as a rule based on the linearization of the time dependence of the gas motion equations [5]. The values of the parameters on the unknown time layer ( $n + 1$ ) are presented in the following form:

$$\vec{F}(\vec{u}^{n+1}) \approx \vec{F}(\vec{u}^n) + \frac{\partial \vec{F}}{\partial \vec{u}}(\vec{u}^n) \Delta \vec{u}$$

$$\text{Here, } \Delta \vec{u} = \vec{u}^{n+1} - \vec{u}^n, \quad (\partial \vec{F} / \partial \vec{u})(\vec{u}^n)$$

is an approximation of the Jacobi matrix that is calculated by the parameters on a known time layer  $\vec{u}^n$ . As a result, the approximation of the motion equations is reduced to a system of linear algebraic equations (LE) in increments of parameters  $\Delta \vec{u}$  (the implicit scheme in the delta form) [8]. In the case of solving the three-dimensional (3D) Navier–Stokes and Reynolds equations, the matrix of such a LE is block-banded with several nonzero block diagonals

and numerous zero diagonals between them. The available methods of solving such a LE can be grouped into two large classes.

In the first class of methods, the LE for  $\Delta\bar{u}$  is not simplified. Several time steps with the exact solution of the LE for infinite time steps are equivalent to the solution of a nonlinear stationary system of equations by Newton's method. This provides the quadratic convergence rate if a close initial approximation is available [9]. However, as a rule, the initial field strongly differs from the solution; therefore, the iteration process has to be started from small time steps. In the case of a LE exact solution, the required computational resources are unacceptably large [5]. Various versions of the conjugate-gradient method are quite common [9], [10]. Among them, the generalized method of minimal residuals (GMRES) [11] in the matrix-free implementation [12] is the most efficient. However, in the general case, the application of different preconditioners [13] is of decisive importance for such methods. When solving ill-conditioned industrial problems, these methods do not ensure sufficient robustness [13].

The methods of the second class, based on the LE simplification, are easier to implement. Here, the methods of factorization can be outlined, which are related to the representation of the matrix of the system of equations in the form of a product of several special-type matrices, as well as the methods related to the representation of the matrix of the system of equations as a sum of several matrices. The high-performance scheme of the first group was proposed in [14]. This is the so-called method of alternating directions (ADI). In this method, the system matrix factorizes into three multipliers associated with the numerical differentiation in each of the spatial directions. Each multiplier reduces to the system, solved by the block Thomas algorithm or even by a series of scalar Thomas algorithm. However, the ADI method in the 3D case is conditionally stable. There are other ways of factorization that are absolutely stable (see, for example, [15]). In the second group of schemes, based on the simplification of the matrices of the system of equations, efficient methods of solving the LE, such as the Jacobi

and Gauss–Seidel block methods [16], are applied, as well as relaxation methods, among which the lower/upper symmetric Gauss–Seidel (LU-SGS) methods and its modification, the lower/upper symmetric successive over relaxation (LU-SSOR) method [17] are especially popular. As a rule, the iteration process for these methods in each time step is broken [5]; therefore, the solution of a simplified LE has not been found. This does not prevent the process of convergence in general to a stationary solution. In contrast to the first-group methods, these methods are easily generalized to unstructured CFD grids [18]. The orientation of the cells in a structured CFD grid may change, which results in better convergence of the Gauss–Seidel method. In the case of unstructured grids, better convergence can be achieved by arbitrary renumbering of the computational cells [19].

In the process of implicit scheme LE simplification, diminishing of the scheme stencil on the implicit layer is of the essence. The delayed correction method [20] is the most common one used for this purpose. In this method, the implicit operator applied to  $\Delta\bar{u}$  is a first-order approximation in space on a compact stencil. The high-order approximation on an expanded stencil is only applied to the explicit operator. The delayed correction method is based on the fact that the implicit operator tends to zero when approaching the stationary solution. This ensures a high order of approximation of the stationary solution. Application of first-order approximation implicit operator improves the scheme reliability.

The implicit method, proposed in the present work, is based on the delayed correction method and applies the Gauss–Seidel block method with the cell renumbering to solve the system of linear equations. This method carries on the traditions of the Russian CFD school, founded by S. K. Godunov and his followers, in particular, A. N. Kraiko and S. M. Bosnyakov. Application of the mathematical properties of the PDE in its approximation, which takes into account the information propagation direction, is the key principle of this school. In the [21]

explicit scheme, the Riemann problem solution was used for this purpose for the first time.

The problem of the choice of approximation of the sources, associated with the production and dissipation of turbulence, arises when constructing the implicit methods for solving the Reynolds equations, closed by the differential model of turbulence. The implicit approximation is quite often used for this purpose. However, it is known that the implicit approximation is not always stable [5]. An absolutely stable scheme was proposed in [22], according to which the explicit approximation was applied for turbulence production, and the implicit scheme was applied for turbulence dissipation. Another method is used in the present work. The method is based on the analysis of eigenvalues of the Jacobi matrix for the sources. This method was first formulated by the author as the logical development of the ideas stated in [23]. Furthermore, the author found that a similar approach had been proposed in the works, where it had been stated that this method guaranteed better convergence than that of [22].

The local choice of an explicit or implicit scheme and the manner of time step implementation (global or local), depending on the relationship between the specified global time step and the local stability condition of the explicit scheme, is the main specific feature of this numerical method. The combined approach allows significant acceleration in obtaining the stationary solution compared to methods that use the same scheme in the entire computational domain. It should be noted that there is a large class of domain decomposition methods [24] in which different numerical methods are applied in different blocks of the computational grid. In contrast to the methods of this class, the choice of the scheme in the proposed approach is determined in each cell of the grid on the basis of numerical solution local parameters, with the algorithm uniformity being kept. The local choice of the scheme ensures the method has high flexibility. The efficiency of this approach is demonstrated through a number of test problems. The implicit scheme and test results were described more carefully in the paper [25].

### 3 Aerodynamics investigations using developed method

In the present paper, two promising integrated configurations are investigated: over fuselage-mounted engines (Figure 2) and the configuration with distributed propulsion, located in the wing (Figure 3). Such configurations make it possible to shield propulsion noise by airframe components.

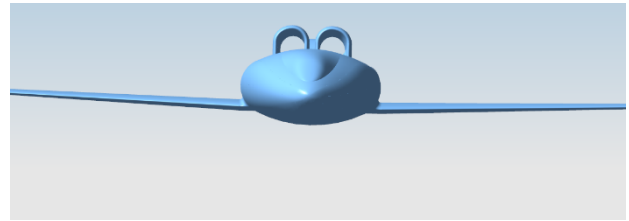


Figure 2 – over fuselage-mounted engines configuration

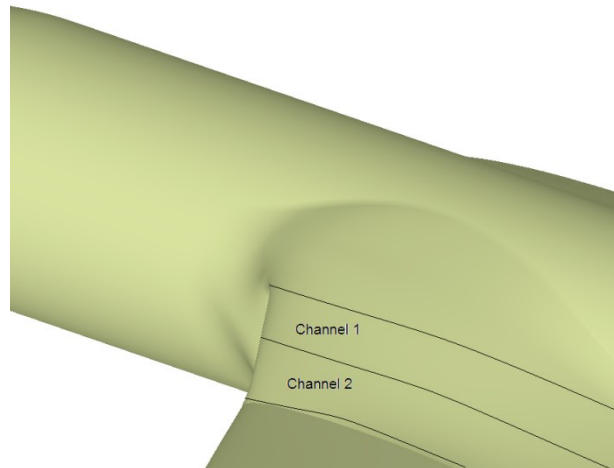


Figure 3 – the configuration with distributed propulsion, located in the wing

#### 3.1 Over fuselage-mounted engines configuration

Configuration of airframe with two engines placed directly on fuselage tail (Figure 2) characterized by following features:

- + aerodynamic efficiency
- + airframe shield engine noise
- + absence of foreign particles from runway hitting into engine
- close displacement engines to each other (interaction, safety)

**COMPUTATIONAL METHOD FOR STEADY FLOW (RANS) USING ZONAL APPROACH AND ITS IMPLEMENTATION EXPERIENCE FOR SOLUTION OF TASK OF INTERFERENCE ENGINE AND AIRFRAME**

- flow disturbances from fuselage can go into engine entrance
- inconvenient airfield service of engine

Wide fuselage usage allows getting additional lift, including at the expense of possibility of high aspect ratio wing usage. Moreover aerodynamical effectiveness such configuration are conditioned that comparing with classical configuration there is no negative wing and engine interference. There is possibility of design of a wing with laminarization of upper and bottom surface with such configuration. Effect of partial boundary layer catching from fuselage positively affected on aerodynamics effectiveness too.

Several different variants of engine displacement must be considered for minimization of negative effects (Figure 4). Engines can be placed on a same distance from each other or together (in a packet). Let us consider features of such variants.

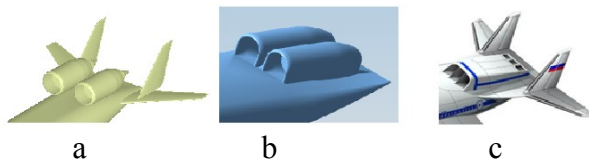


Figure 4 – different variants of engine design

$R$  – distance between nacelles  
 $D_{mid}$  – nacelle midship diameter  
 $R \sim D_{mid}$  (Figure 4 a):

- + inlets interaction is low
- + no problems in the fan blade expansion
- increased negative interference of two nacelles to each other
- big weight

$R \ll D_{mid}$  (Figure 4 b):

- + low negative interference of two nacelles to each other
- + no problems in the fan blade expansion
- presents inlets interaction

$R = 0$  (Figure 4 c):

- + one nacelle (no negative interference)
- + low weight
- strong inlets interaction
- problems in the fan blade expansion

We have identified the main characteristics of the studied configuration. Let us consider the characteristics of the power plant inlet for different variants of this configuration. Firstly, we consider the characteristics of the inlet for high wing with engines mounted directly on the fuselage.

The main characteristic of the air intake is the total pressure recovery coefficient  $\sigma$ . The first stage of the work is the optimization of the inlet for providing acceptable values of the coefficient  $\sigma$  on the takeoff and landing regimes (Figure 5). In terms of thrust characteristics optimal variant (variant 2) better then base (variant 1) by 3-4%. All characteristics are at a mass flow rate equal  $q(\lambda)_{eng} = 0.72$ . It should be noted that under the classical configuration (Figure 5) refers to the power plant nacelle mounted on the pylon under the wing. The engine works in such a case, basically, in the undisturbed flow, i.e. under conditions without getting the boundary layer from the aircraft airframe elements.

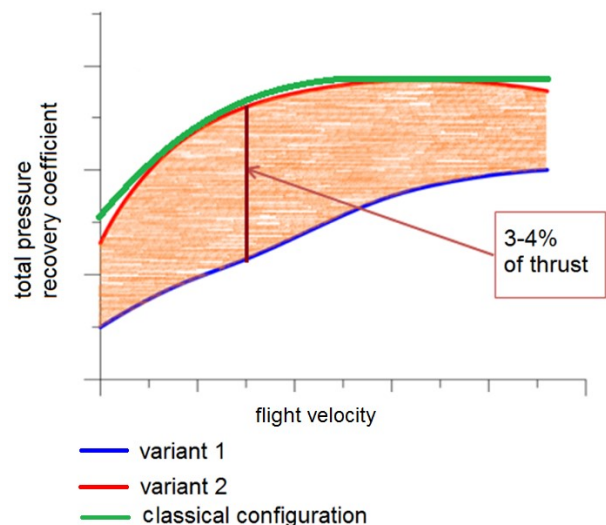


Figure 5 – result of inlet geometry optimization

At numbers  $M \leq 0.4$  the coefficient  $\sigma$  value obtained at level of standard dependence. With increasing of number  $M > 0.4$  the coefficient  $\sigma$  value decreases. However, the total value of the total pressure distortion of flow in the channel at the considered Mach numbers range (up to  $M = 0.8$ ) does not exceed the regulation value.

In experimental investigations and computations for takeoff and landing regimes and angles of attack  $\alpha \leq 5^\circ$  unseparated flow is observed even at sideslip angle  $\beta = 10^\circ$  and  $\beta = 15^\circ$ . Beginning of separated flow occurs at the junction of the wing and fuselage. At the angle of attack  $\alpha = 10^\circ$  local vortex flow occurs in the upper part of the fuselage in the region of the junction of the wing and fuselage. However, vortex and separation zone pass intakes. At all considered regimes by  $\alpha$  and  $\beta$  at  $M = 0.25$  level of the total pressure losses in the inlet entrance is very low ( $\sigma \approx 0.995$ ).

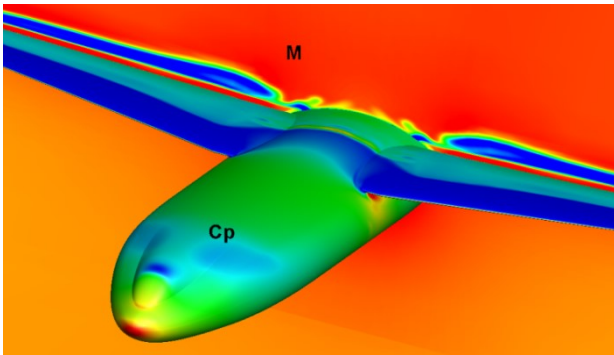


Figure 6 – flow field after wing. Number  $M = 0.8$

Consider causes of flow characteristic downgrade in the inlet entrance at high speeds (the number  $M = 0.8$ ). Studies with this number  $M$  formed at different angles of attack. At angles of attack  $\alpha = 2.5^\circ$  and  $\alpha = 5^\circ$  flow over the upper surface of the airframe, mainly occurs without flow separation zones. But at the same time, there are areas of the fuselage boundary layer thickening and closed local vortex zones near the top surface of the fuselage. Total pressure losses in the engine inlet connected with these effects. The local vortex zones formed at the junction of the wing and fuselage (Figure 6).

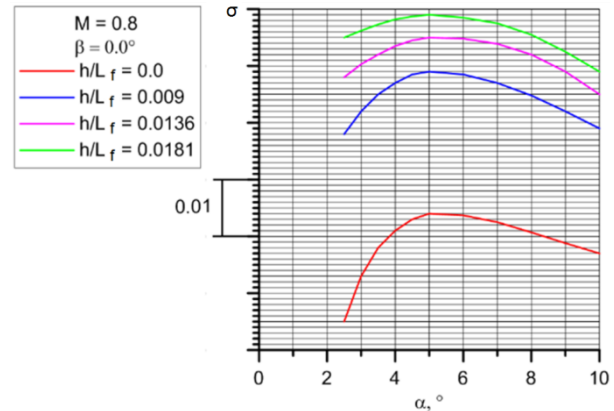


Figure 7 – dependence of coefficient  $\sigma$  from angel of attack with different engine mounting high

If the number  $M = 0.8$  the coefficient  $\sigma$  value considerably depends on the angle of attack (Figure 7). The maximum value of  $\sigma$  is obtained when the angle of attack  $\alpha = 5^\circ$ . To clarify the physical nature of the obtained dependence at  $M = 0.8$  a more detailed analysis of the flow field in front of the intake is made. The region occupied by the boundary layer with low total pressure is greatest precisely when the angle of attack  $\alpha = 2.5^\circ$ . It is connected with the overflow of the boundary layer from the bottom surface of the fuselage on its upper surface.

At an angle  $\alpha = 5^\circ$  on the fuselage surface from the outside intake it is a "contraction" (ejection) of the boundary layer from intake due to the formation of secondary vortex flows and their ejection effect. Area of low total pressure flowing into the intake is reduced. As a result, the average value of the total pressure at inlet increases.

At the angle of attack  $\alpha = 10^\circ$  even greater effect removal of the boundary layer at the side of the inlet is observed. However, in this case portion of vortex flow with a low total pressure begins to fall in the intake entrance, which leads to a reduction of coefficient  $\sigma$  as compared to its value at  $\alpha = 5^\circ$ .

Obtained characteristics of a power plant located directly on the surface of the fuselage satisfy the norm for stable power plant operation. However, as stated earlier, it is necessary to reach the minimum values of the total pressure losses to reduce fan noise and to obtain a minimum loss of engine thrust.

Below (Figure 8) results of numerical calculations of coefficient  $\sigma$  for  $M=0.8$  by different distance of the intake from the fuselage surface on the values  $h = h/L_f = 0 \div 0.0018$  are presented. In this case, at  $\bar{h} \sim 0.01$  the flow characteristics in the plane of the entrance are significantly increased. The area of low total pressure is greatly reduced. With an increase of the relative magnitude  $\bar{h} = h/L_f$  coefficient  $\sigma$  increases significantly.

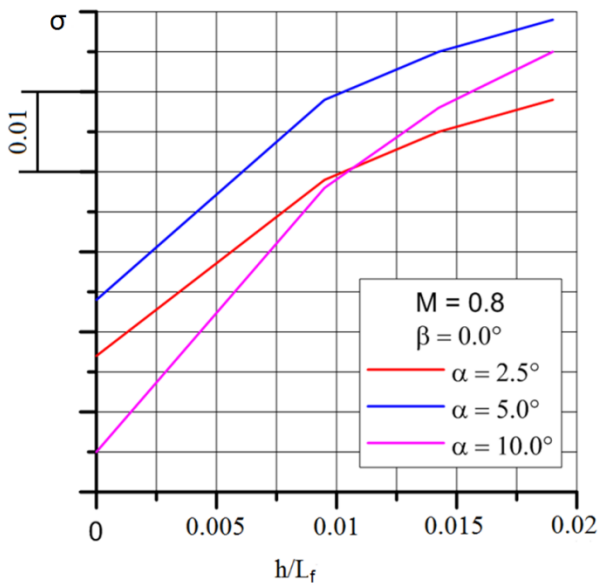


Figure 8 – dependence of the total pressure recovery coefficient on the height of the engine displacement

Optimum flight regime for the coefficient  $\sigma$  is flight mode at  $\alpha = 5^\circ$ . At this mode, maximum total pressure recovery coefficient realized at all considered intake heights from the fuselage.

Consider the effect of wing installation (high wing, low wing) on flow at front air intake. At a low wing location flow field is significantly more favorable compared with one at high wing, especially when the angle of attack  $\alpha = 2.5^\circ$ .

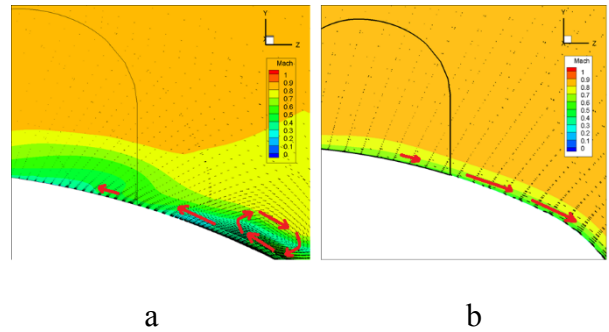


Figure 9 – flow field before intake. a – high wing, b – low wing

Consider the Mach number field for the two variants for installing the wing on the fuselage (Figure 9). Arrows on these figures show the direction of the flow. In the version with the lower wing largely manifested positive effect of the fuselage boundary layer contraction due to the vortex flow of wide fuselage. The dimensions of the boundary layer (i.e. the low total pressure area) in the intake for the lower-wing variant is considerably less than in the upper-wing variant, especially in the angle of attack  $\alpha = 2.5^\circ$ . Positive effect of the boundary layer contraction is due to vortex flow generated on the fuselage side, the trace of which is shown at the bottom right side of the figure (Figure 9 a).

From the analysis results of the obtained materials it follows that in terms of intake operations more favorable aircraft design is with lower position of the wing on a wide fuselage.

Another problem that arises while the designing of wide-body aircraft with engines mounted behind is an interference of engine nacelles with each other. Their resistance at cruising flight increases when placing the engine at a small distance from each other. Consider the flow around nacelles with a duct on different regimes.

At high flow velocity ( $M \sim 0.8$ ) in the case of an isolated nacelle (Figure 10) flow is quiet with little shock on the outer nacelle surface. In the case of two nacelles placed on a distance  $D=0.8$  (distance is related to the diameter of the midsection of the nacelle) flow qualitative changed (Figure 11). Flow accelerates between two nacelles. Acceleration closed by shock wave and the boundary layer separation formed from under of shock. These

factors lead to a dramatic increase in the resistance of the engine nacelles. At Mach number  $M = 0.82$  resistance increases about twice. Interference resistance decreases with increasing distance between the nacelles.

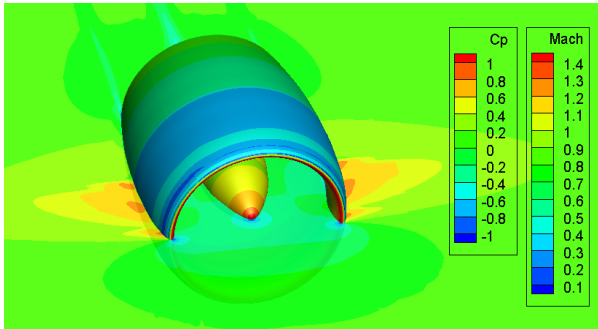


Figure 10 – flow field near isolated nacelle

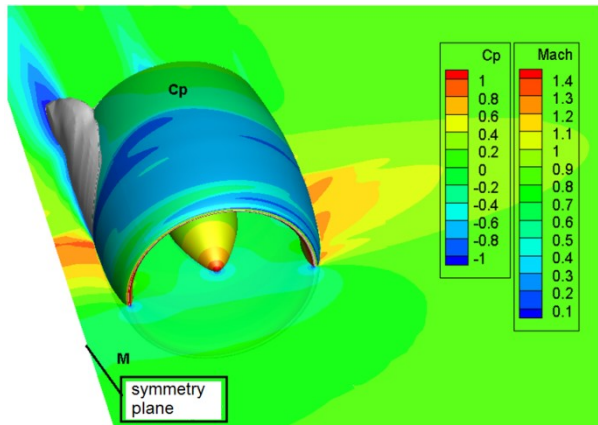


Figure 11 – flow field near nacelle in second presence

### 3.2 The configuration with distributed propulsion, located in the wing

One of the most interesting but not enough studied integrated configurations of power plant is deeply integrated with the airframe configuration with in wing mounted distributed engine (Figure 3). Features of this scheme are the following:

- + a smaller cross-sectional area at the location of the engine
- + engine noise screened by airframe
- + small fan noise level by increasing the channel length
- proximity of the engine channels to each other (interaction, security)
- disturbance from the fuselage

At the same time unconventional configuration deeply integrated propulsion systems require detailed computational and experimental research and study both input and output systems. One of the main issues of configuration under consideration in terms of the power plant is hitting the boundary layer formed on the fuselage front to the intake entrance.

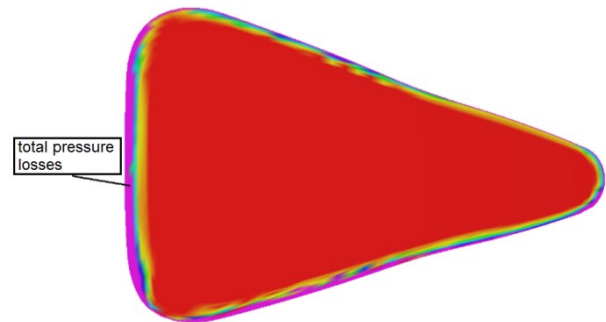
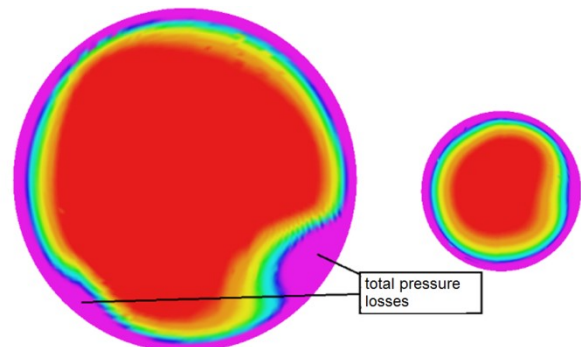


Figure 12 – field of total pressure recovery coefficient at the intake entrance.  $M = 0.82$ ,  $\alpha = 2.5^\circ$



Channel 1

Channel 2

Figure 13 – field of total pressure recovery coefficient at two channels.  $M = 0.82$ ,  $\alpha = 2.5^\circ$

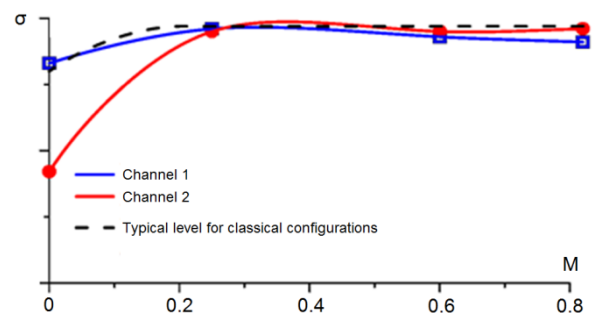


Figure 14 – dependence of total pressure recovery coefficient  $\sigma$  for two channels by Mach number

Let us consider field of total pressure recovery coefficient at the intake entrance (Figure 12) and at the engine entrance (Figure 13) at Mach number  $M = 0.82$ . At cruise Mach number total pressure losses is present due to the boundary layer in the region adjacent to the fuselage. Because of the relatively small area of losses it has small effect on the averaged value of the coefficient  $\sigma$  (Figure 14). At cruise flight ( $M = 0.82$ ,  $\alpha = 2.5^\circ$ ) high average values of the coefficient  $\sigma$  achieved for both channels. On takeoff and landing speed ( $M = 0.25$ ) effect of boundary layer is practically absent.

High intake characteristics remain in range of angles of attack  $\alpha = 0 \div 5^\circ$  for channel 1 and at  $\alpha = 0 \div 10^\circ$  for channel 2. By increasing the angle of attack up to  $\alpha = 10^\circ$  at cruise Mach number ( $M = 0.82$ ) flow separation forms at the intake bottom. Separation produced by changing the flow direction associated with the wash from the fuselage in combination with a large angle of attack. The separation results in a decrease in the coefficient  $\sigma$  of channel 1. The separation has no effect on flow in the channel 2.

An important results were obtained on the effect of intake throttling on their characteristics at cruise Mach number  $M = 0.82$  and angle of attack  $\alpha = 2.5^\circ$ . Characteristics of total pressure recovery coefficient remain high at throttling of the 1st and 2nd channels intake. In this case, flow without separation is in channel 2. For channel 1 (as at regimes without throttling) area of low total pressure remains in the region located near the fuselage.

The size of the area with total pressure losses slightly increased compared with the regime without throttling. It is a consequence of the interaction of the flow with the boundary layer.

Regime of a low-speed ( $M = 0.25$ ) and a large angle of attack  $\alpha = 10^\circ$  is interesting. In this regime, the same separation is formed. For the given parameters of the engine, there is overflow stream from the channel 2 to channel 1. Because of this, the flow separation generated on the channel 1 side far from the fuselage. However, it closed and has a local character.

Flow on regime at  $M = 0$  (Figure 15) has similar nature. Flow wash by sideslip angle  $\beta$  forms before the intake. Flow separations are

formed on the side surfaces of the channels. But in this case, the effect is not a local and separations distributed throughout the length of the channels. This regime is the most intensive of all investigated ones, especially for channel 2. A low pressure area occupies a large part of the cross section of the channel 2. The gas-dynamic stability of the engine may become worse. Flow separation forms in the beginning of the channels on the side far from the fuselage.

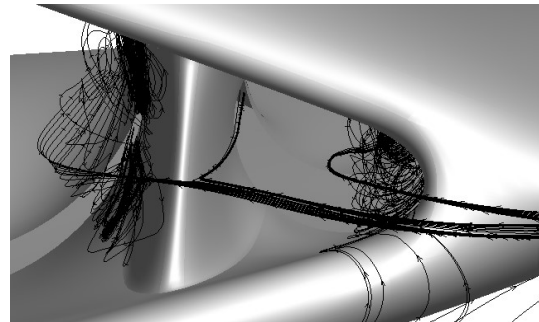


Figure 15 – flow separation at  $M = 0$

Let us consider the coefficient  $\sigma$  values depending on the flight Mach number compared to typical values for classical configuration of nacelles mounted on pylons under the wing of the plane (Figure 14). On most regimes coefficient of total pressure recovery for investigated configuration with intakes in a wing close to typical values (difference is less than 0.5 %). A high stability characteristics for the angle of attack up to investigated values  $\alpha = 10^\circ$  both takeoff ( $M = 0.25$ ) and cruise ( $M = 0.82$ ) aircraft velocity is obtained. The smallest value (below standard level) of coefficient  $\sigma$  obtained only at regime  $M = 0$  for the intake of the channel 2.

#### 4 Conclusions

1. A combined method based on the Godunov–Kolgan–Rodionov scheme has been proposed. The method combines the local application of the implicit scheme with a prescribed global time step in the vicinity of surfaces with a no-slip condition, the explicit scheme with the local time step in regions where the prescribed time step does not exceed

the stability condition of the explicit scheme, and the implicit scheme with the local time step in buffer regions distant from the considered body.

2. Configuration with the engines mounted on the fuselage:

- It is shown that at angles of attack close to cruise value (from  $\alpha = 0$  to  $\alpha = +5^\circ$ ) and at zero sideslip angle ( $\beta = 0$ ), sufficiently high (taking into account the boundary layer of the fuselage) total pressure recovery coefficient  $\sigma$  and low values of the total flow distortion in the intake channel are obtained
- At number  $M = 0.4$  angle of attack change in the investigated range from  $\alpha = -5^\circ$  to  $\alpha = 15^\circ$  and sideslip angle change from  $\beta = -5^\circ$  to  $\beta = 5^\circ$  have little effect on intake characteristics
- Angle of attack and sideslip angle effects on intake characteristics increases at Mach number from  $M = 0.6$  to  $M = 0.8$

3. The configuration with distributed propulsion located in the wing:

- It is shown that for developed variants wing intakes two channels distributed turbofan power plant located in the wing, high performance of the total pressure recovery coefficient  $\sigma$  can be provided at the level of typical values for traditional nacelles configuration located on pylons under the wing of an airplane.
- It is established that on the most of considered flight regimes smooth flow of intakes and channels is realized without flow separation. On intake of channel 1 a small area of lower total pressure on the side adjacent to the fuselage is observed. It associated with the overflowing to the channel 1 portion of the boundary layer grown on the fuselage surface. The region of lower total pressure is practically absent in the entrance section of channel 2, it is a favorable factor for high gas dynamic stability of the power plant.
- When you increase the angle of attack up to  $\alpha = 10^\circ$  at cruising flight ( $M = 0.82$ ) in the bottom of the intake entrance formed a local flow separation. In the channel 2 flow separation has little effect on the value  $\sigma$ .
- On takeoff regime ( $M = 0.25$ ) high performance intake characteristics are remained for two channels in all range of angles of attack

$\alpha = 0 \div 10^\circ$ . But at an angle of attack  $\alpha = 10^\circ$  at the intake entrance flow from channel 2 to channel 1 is observed. Because of this, the flow separation generated on the far from the fuselage side of channel 1. However, it is closed and has a local character.

- High flow characteristics of intake channels at investigated regimes ( $M = 0.82$  and angle of attack  $\alpha = 2.5^\circ$ ) remain after intakes throttling. At engine operation on site ( $M = 0$ ) at the intake entrance are formed wash by sideslip angle. Due to this flow separation appear on the channel side farthest from fuselage. Separation zone extend over the entire length of channels. This regime is the most intensive of all investigated ones.

## References

- [1] Neyland V. Ya., Bosniakov S. M., Glazkov S. A., Ivanov A. I., Matyash S. V., Mikhailov S. V. and Vlasenko V. V., Conception of electronic wind tunnel and first results of its implementation, *Prog. Aerosp. Sci.*, vol. 37, pp. 121–145, 2001.
- [2] Bosniakov S. M., Vlasenko V. V., Kursakov I. A., Mikhailov S. V., and Quest J., Problem of interference of an ogival body of revolution with the wind-tunnel sting and specific features of computing this problem, *TsAGI Sci. J.*, vol. 42, no. 3, pp. 321–344, 2011.
- [3] Engulatova M. F. and Matyash S. V., Software package EWT—Program implementation of aerodynamic experiment technology, *Proc. of 18th TsAGI School Workshop on Aircraft Aerodynamics*, 2007 (in Russian).
- [4] Vlasenko V. V. and Mikhailov S. V., ZEUS program for calculating the unsteady flows in the frame of RANS approach, *Proc. of TsAGI 18th School Workshop on Aircraft Aerodynamics*, 2009 (in Russian).
- [5] Blazek J., *Computational Fluid Dynamics: Principles and Applications*, New York: Elsevier, 2001.
- [6] Fedorenko R. P., Multigrid method for the finite-element schemes, *Zh. Vychisl. Mat. Mat. Fiz.*, vol. 1, no. 5, 1961 (in Russian).
- [7] Trottenberg U., Oosterlee C., and Schuller A., *Multigrid*, Cornwall, U.K.: Academic, 2001.
- [8] Yoon S. and Kwak D., Implicit methods for the Navier–Stokes equations, *Comput. Syst. Eng.*, vol. 1, no. 2–4, pp. 535–547, 1990.
- [9] Hestenes M. R. and Stiefel E. L., Methods of conjugate gradients for solving linear systems, *J. Res. Natl. Bur. Stand.*, vol. 49, no. 6, pp. 409–436, 1952.

- [10] Sonneveld P., CGS, a fast Lanczos-type solver for nonsymmetric linear systems, *SIAM J. Sci. Stat. Comput.*, vol. 10, pp. 36–52, 1989.
- [11] Sad Y. and Schulz M. H., GMRES: A generalized minimum residual algorithm for solving nonsymmetric linear systems, *SIAM J. Sci. Stat. Comput.*, vol. 7, pp. 856–869, 1986.
- [12] Zingg D. and Pueyo A., An efficient Newton–GMRES solver for aerodynamic computations, AIAA Paper 97-1955, 1997.
- [13] Venkatakrishnan V., Preconditioned conjugate gradient methods for the compressible Navier–Stokes equations, *AIAA J.*, vol. 29, pp. 1092–1110, 1991.
- [14] Beam R. M. and Warming R. F., An implicit finite-difference algorithm for hyperbolic systems in conservation-law form, *J. Comput. Phys.*, vol. 22, pp. 87–110, 1976.
- [15] Steger J. L. and Warming R. F., Flux vector splitting of the inviscid gasdynamic equations with application to finite-difference methods, *J. Comput. Phys.*, vol. 40, pp. 263–293, 1981.
- [16] Ortega M. J., *Introduction to Parallel and Vector Solution of Linear Systems*, New York: Plenum, 1988.
- [17] Yoon S. and Jameson A., An LU-SSOR scheme for the Euler and Navier–Stokes equations, *AIAA J.*, vol. 26, pp. 1025–1026, 1988.
- [18] Batina J. T., Implicit upwind solution algorithms for three-dimensional unstructured meshes, *AIAA J.*, vol. 31, pp. 801–805, 1993.
- [19] Anderson W. K. and Bonhaus D. L., An implicit upwind algorithm for computing turbulent flows on unstructured grids, *Comput. Fluids*, vol. 23, pp. 1–21, 1994.
- [20] Ferziger J. and Peri M., *Computational Methods for Fluid Dynamics*, 3rd Ed., New York: Springer, 2002
- [21] Godunov S. K., Difference method for numerical computation of discontinuous solutions in hydrodynamics, *Math. Sb.*, vol. 47, no. 3, pp. 271–306, 1959 (in Russian).
- [22] Wilcox D. C., Progress in hypersonic turbulence modeling, AIAA Paper 91-1785, 1991.
- [23] Vlasenko V. V., On a mathematical approach and principles of constructions of numerical methodologies for the software package EWT-TsAGI. Collection of works on the practical aspects of solving the problems of external aerodynamics of aircraft engines in the frame of time-averaged Navier–Stokes equations, *Tr. TsAGI*, vol. 2671, pp. 20–85, 2007 (in Russian).
- [24] Glowinski R., Golub G. H., Meurant G. A., and Periaux J., eds., *Domain Decomposition Methods for Partial Differential Equations*, New York: 1988.
- [25] Kazhan E. V., Stability improvement of Godunov–Kolgan–Rodionov scheme by a local implicit smoother, *TsAGI Science Journal*, Vol. 43, 2013.

## 5 Contact Author Email Address

Lysenkov Alexander, PhD, hade of group:  
tel.: +7 (495) 556-35-16  
mailto:lysenkov@tsagi.ru

## Copyright Statement

The authors confirm that they, and/or their company or organization, hold copyright on all of the original material included in this paper. The authors also confirm that they have obtained permission, from the copyright holder of any third party material included in this paper, to publish it as part of their paper. The authors confirm that they give permission, or have obtained permission from the copyright holder of this paper, for the publication and distribution of this paper as part of the ICAS 2014 proceedings or as individual off-prints from the proceedings.